Electronic Supplementary Information

Amidothiourea based colorimetric receptors for basic anions: evidences of anion induced deprotonation of amide –NH proton and hydroxide induced anion…π interaction with the deprotonated receptors

*Arghya Basu, Sandeep Kumar Dey and Gopal Das**

Department of Chemistry

Indian Institute of Technology, Guwahati

E-mail: gdas@iitg.ernet.in

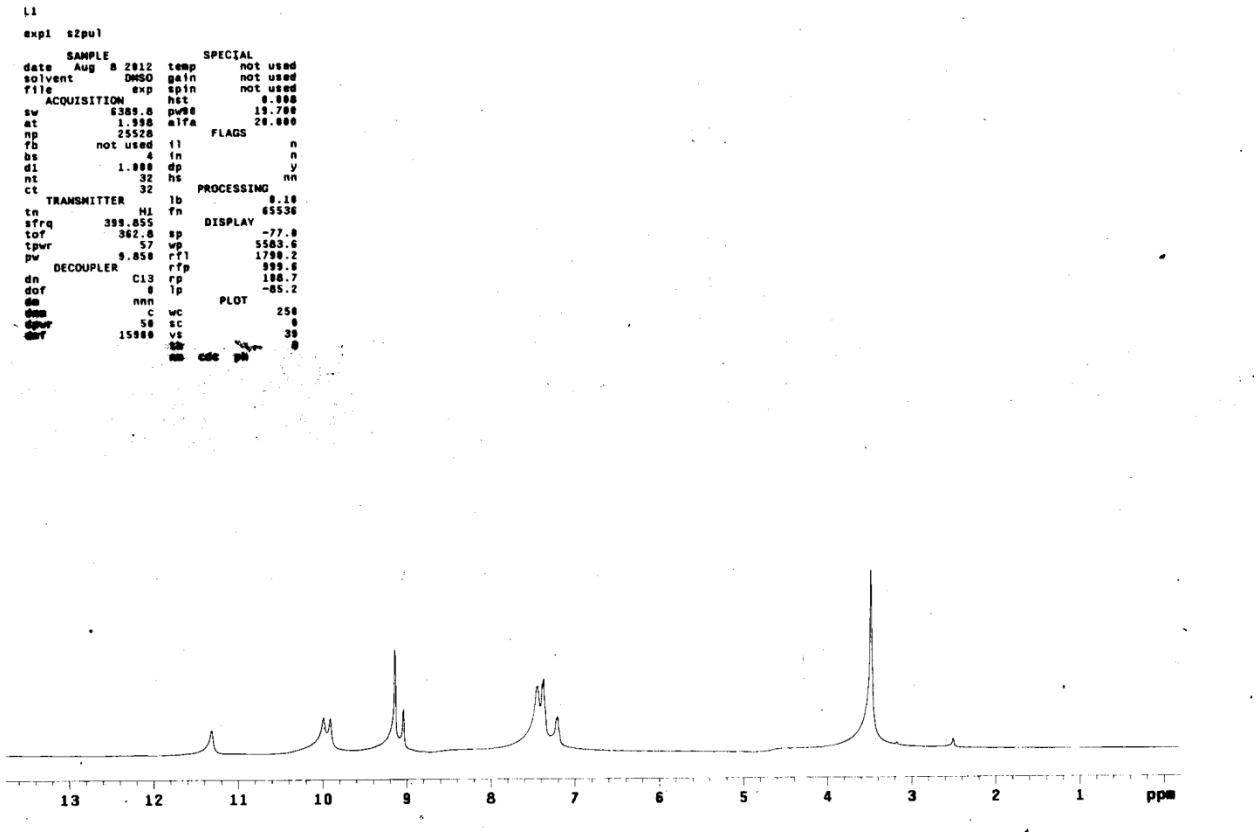

Fig.S1 ^{1}H-NMR spectrum of receptor L1 in d_6-DMSO at 298K.

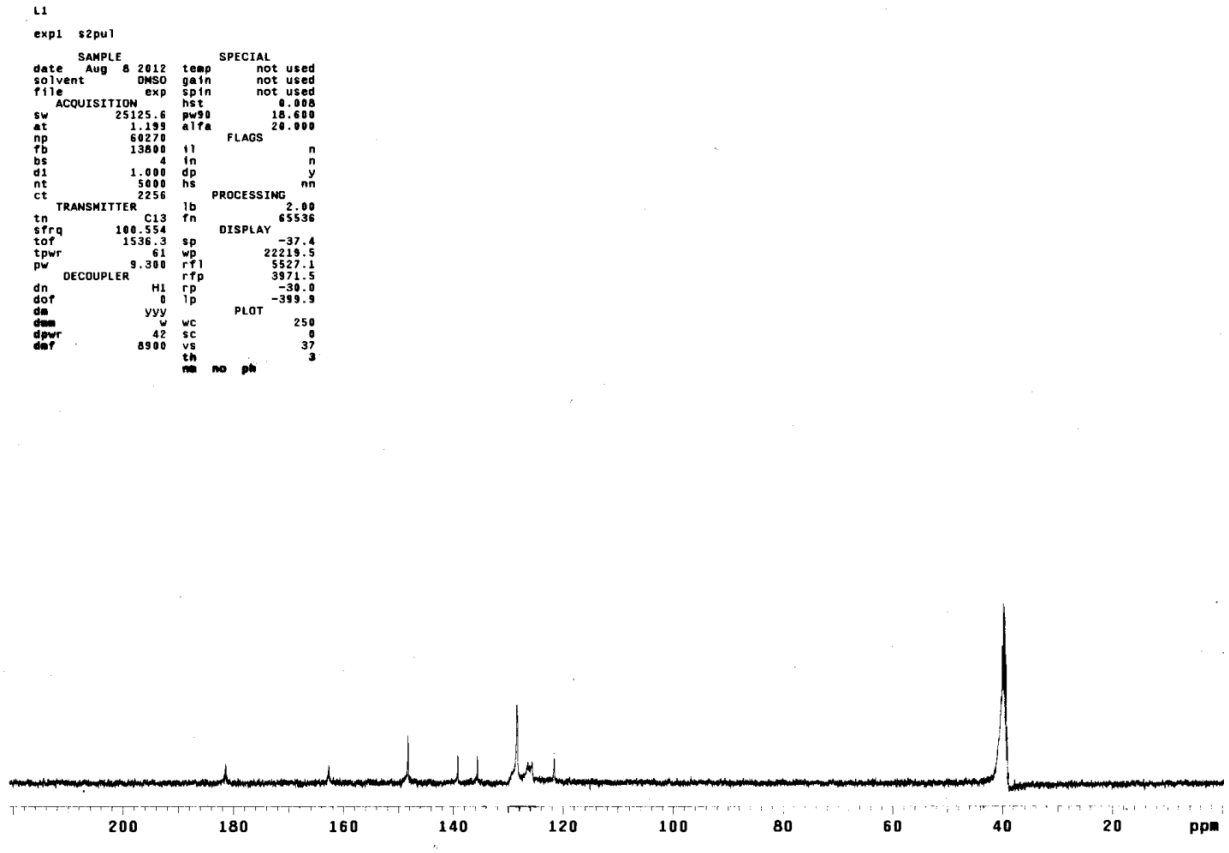

Fig.S2 ^{13}C-NMR spectrum of receptor L1 ind_6-DMSO at 298K.

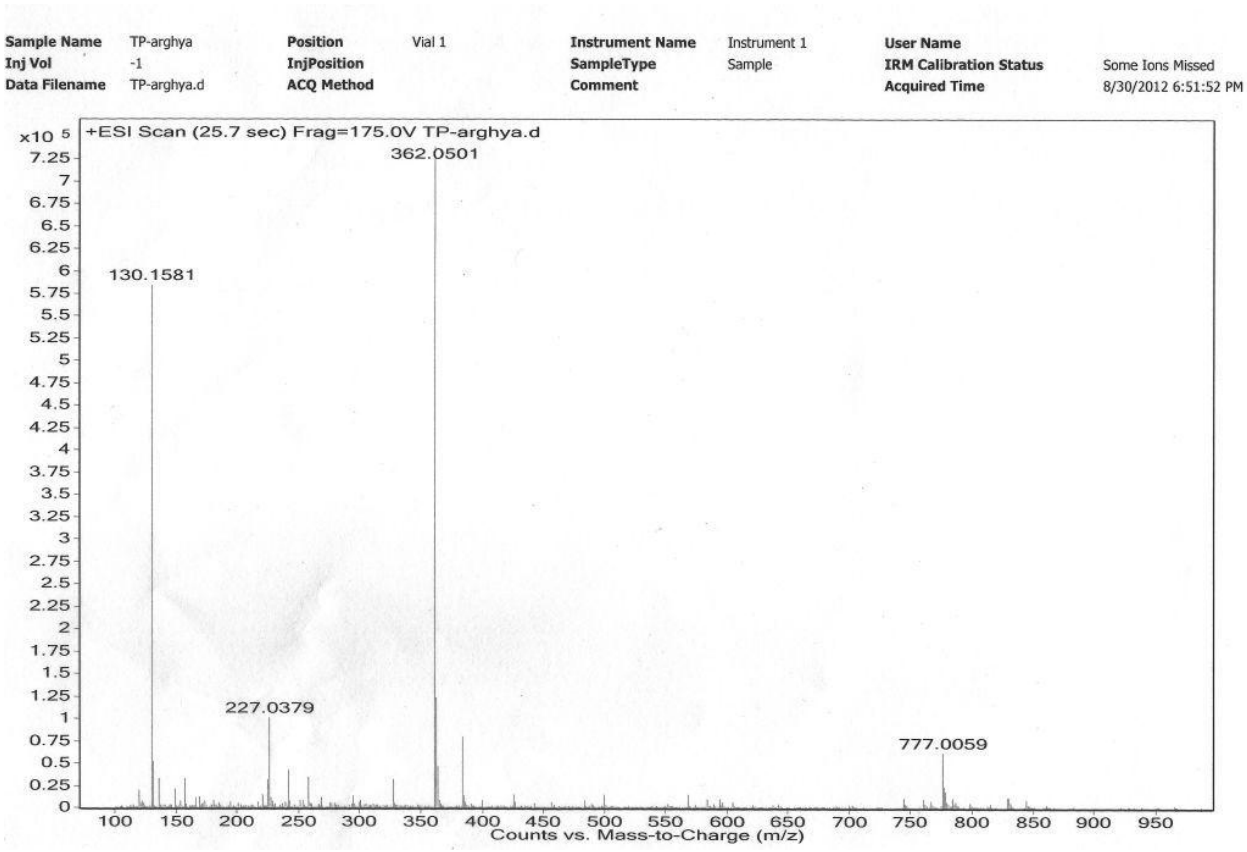

Fig.S3 Mass spectrum of receptor L1 in acetonitrile**.**

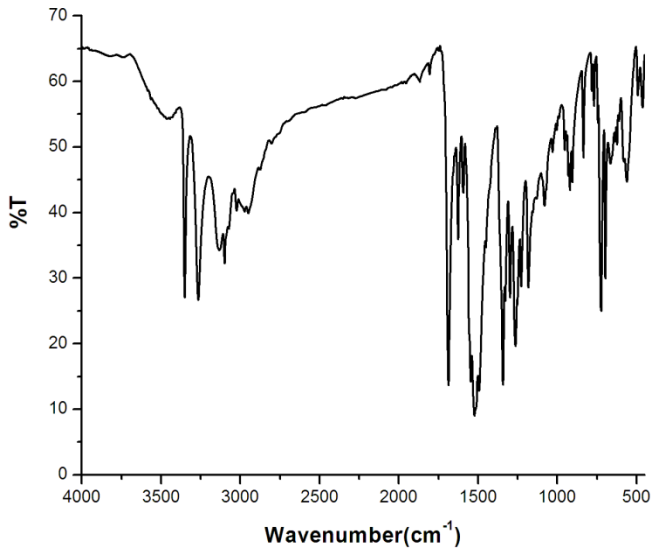

Fig.S4 IR spectrum of receptor L1.

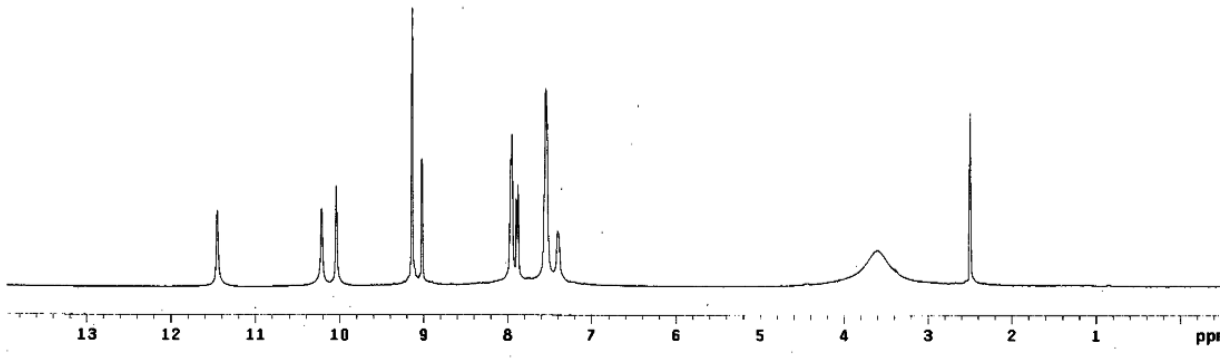

Fig.S5 ^{1}H NMR spectrum of receptor L2 in d_6-DMSO at 298K.

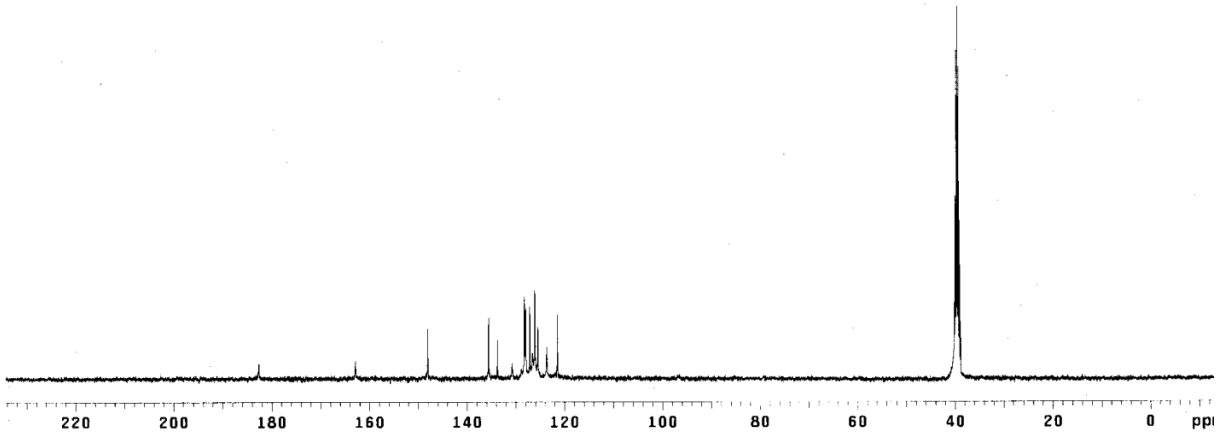

Fig.S6 ^{13}C NMR spectrum of receptor L2 in d_6-DMSO at 298K.

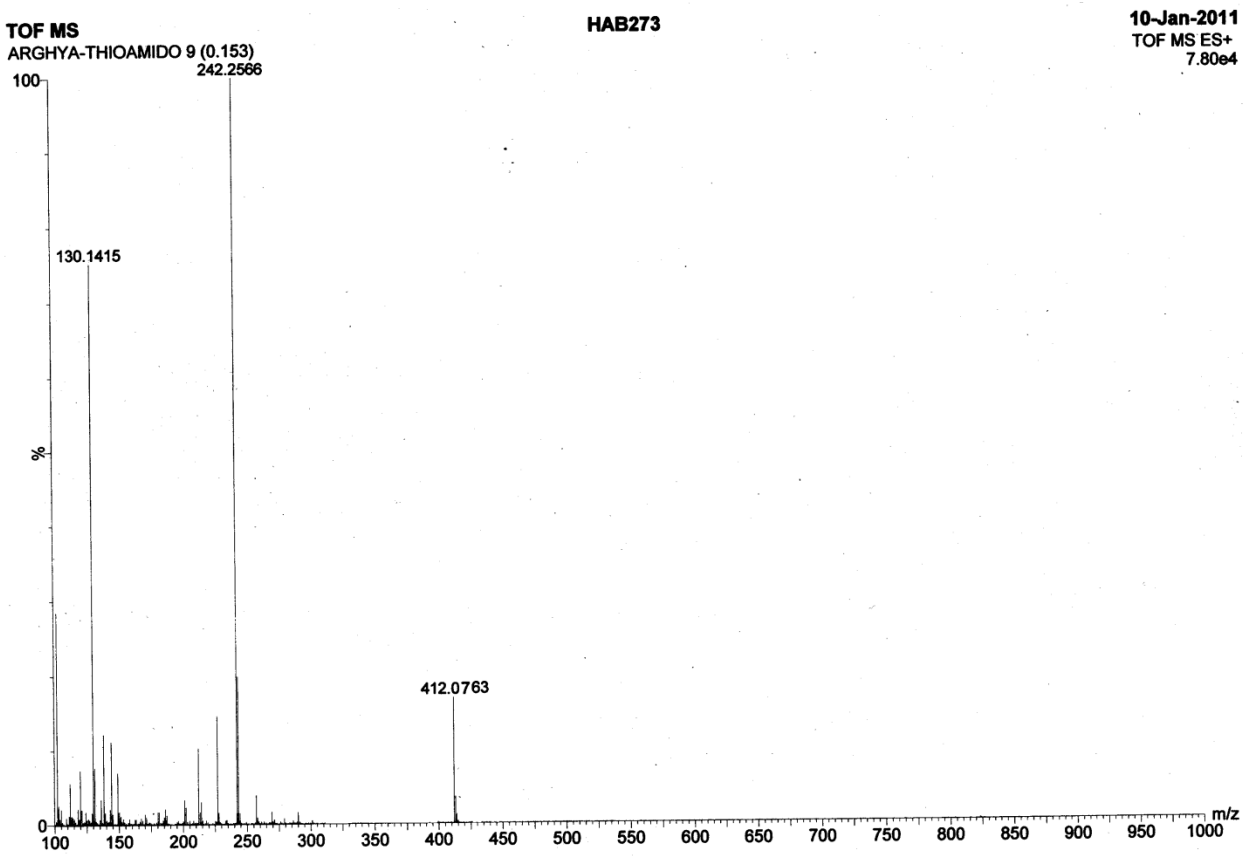

Fig. S7 ESI-Mass spectrum of receptor L2 in acetonitrile**.**

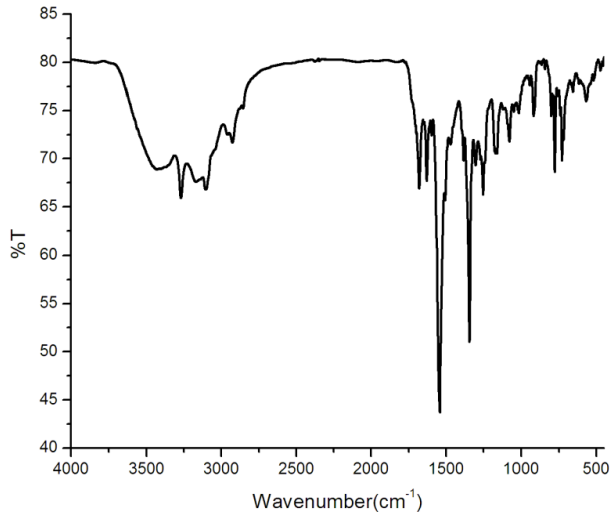

Fig.S8 IR spectrum of receptor L2.

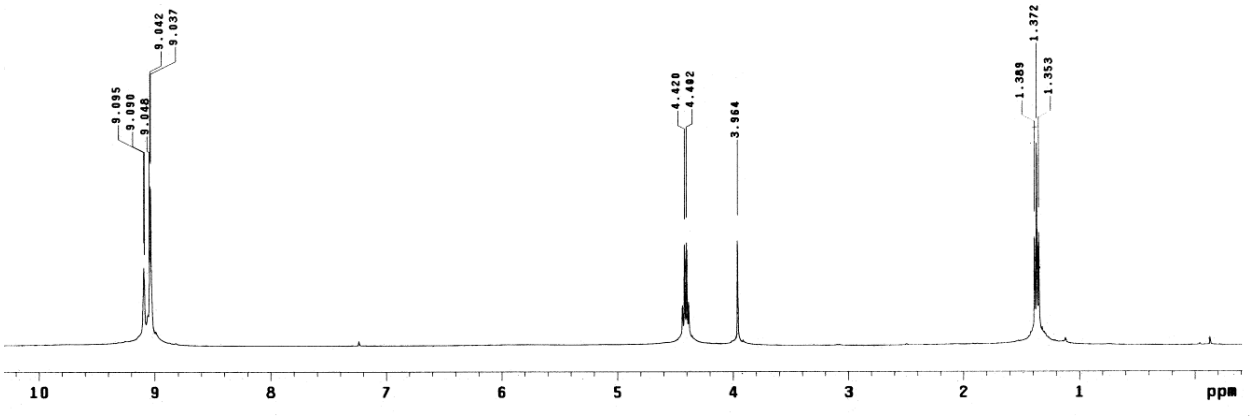

Figure S9. ^{1}H NMR spectrum of control receptor L_C in $CDCl_3$ at 298 K**.** (Figure reproduced from S. K. Dey and G. Das, *Chem. Commun*., 2011, **47**, 4983–4985).

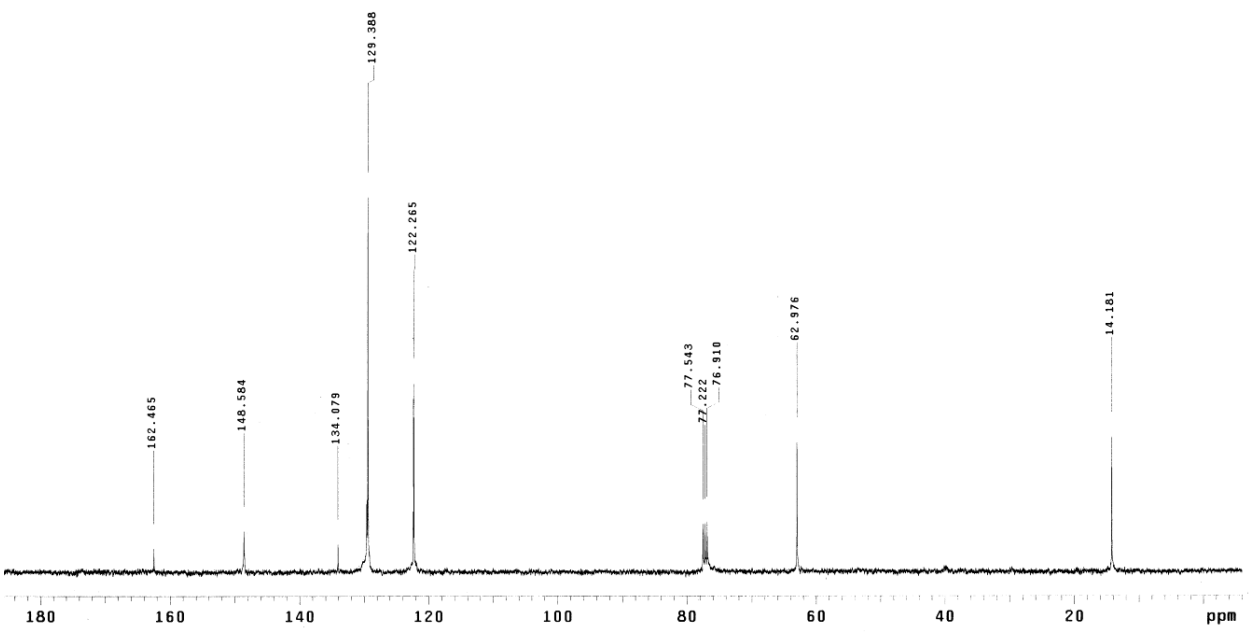

Fig.S10 ^{13}C NMR spectrum of control receptor L_C in $CDCl_3$ at 298K. (Figure reproduced from S. K. Dey and G. Das, *Chem. Commun*., 2011, **47**, 4983–4985).

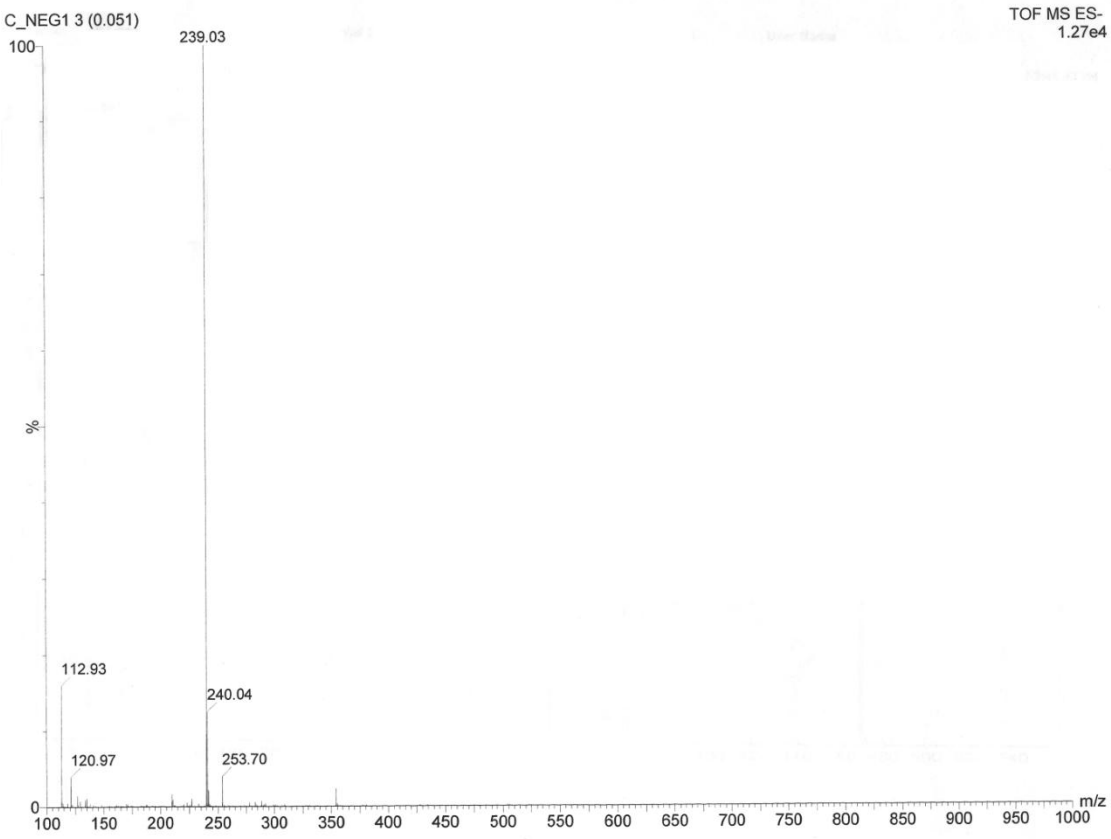

Fig. S11 ESI-Mass spectrum of receptor L_C in acetonitrile**.**

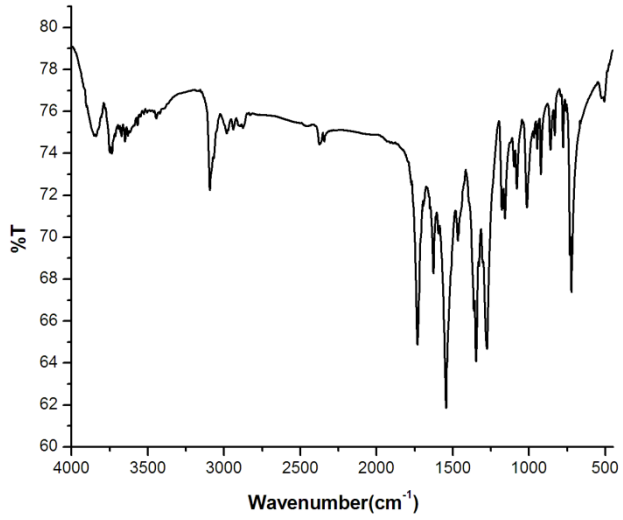

Fig.S12 IR spectrum of receptor L_C.

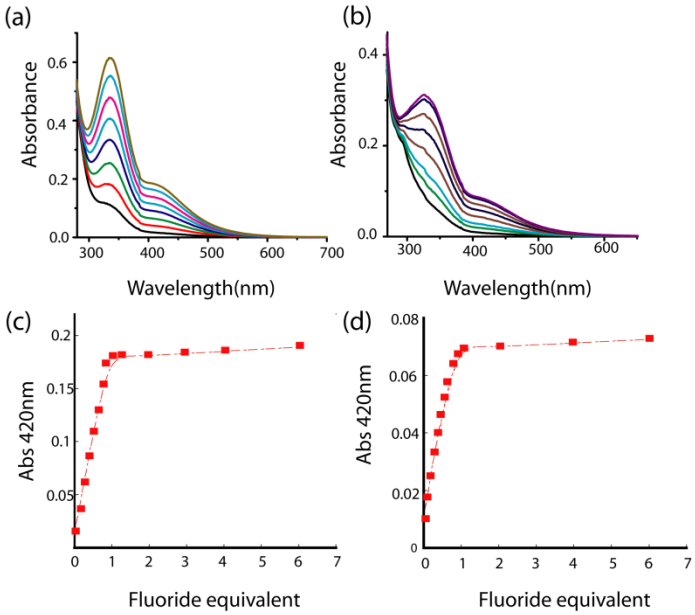

Fig.S13 a) UV−vis titration of the receptor L1 (4.0 x 10^{-5} M) in CH_3CN solution with standard solution of [*n*-Bu_4N]F. (b) The change of UV−vis spectra of the receptor L2 (3.4 x 10^{-5} M) in CH_3CN solution upon gradual addition of standard solution of [*n*-Bu_4N]F. (c) Relative change in the absorption spectra of L1 (4.0 x 10^{-5} M) at 420 nm upon addition of fluoride anions in CH_3CN. (d) Plot of the change in the absorption of L2 upon addition of fluoride in CH_3CN.

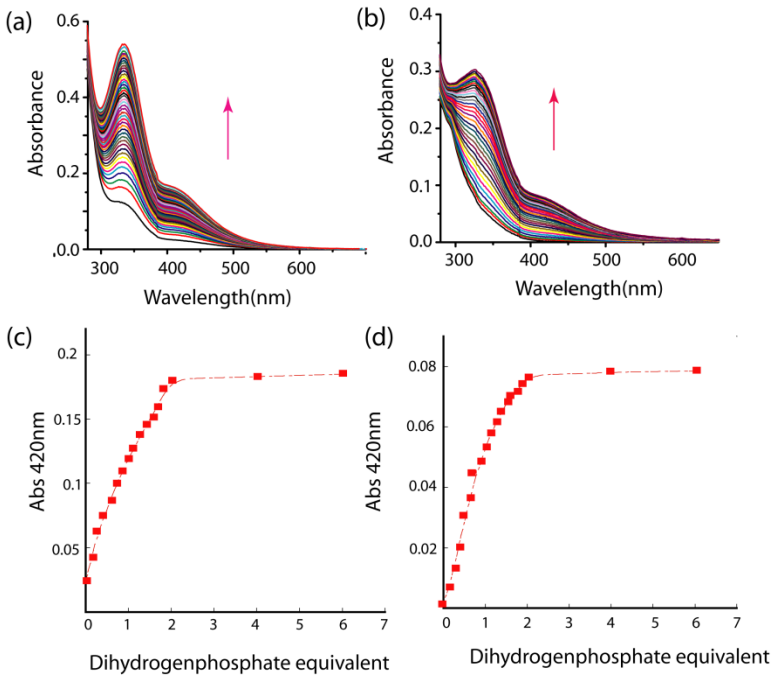

Fig. S14 a) UV−vis titration of the receptor L1 (4.0 x 10^{-5} M) inCH_3CN solution with standard solution of [*n*-Bu_4N]H_2PO_4. (b) The change of UV−vis spectra of the receptor L2 (3.4 x 10^{-5} M) in CH_3CN solution upon gradual addition of standard solution of [*n*-Bu_4N]H_2PO_4. (c)Relative change in the absorption spectra of L1 (4.0 x 10^{-5} M) at 420 nm upon addition of di-hydrogenphosphate anions in CH_3CN. (d) Plot of the change in the absorption of L2 upon addition of di-hydrogenphosphate in CH_3CN.

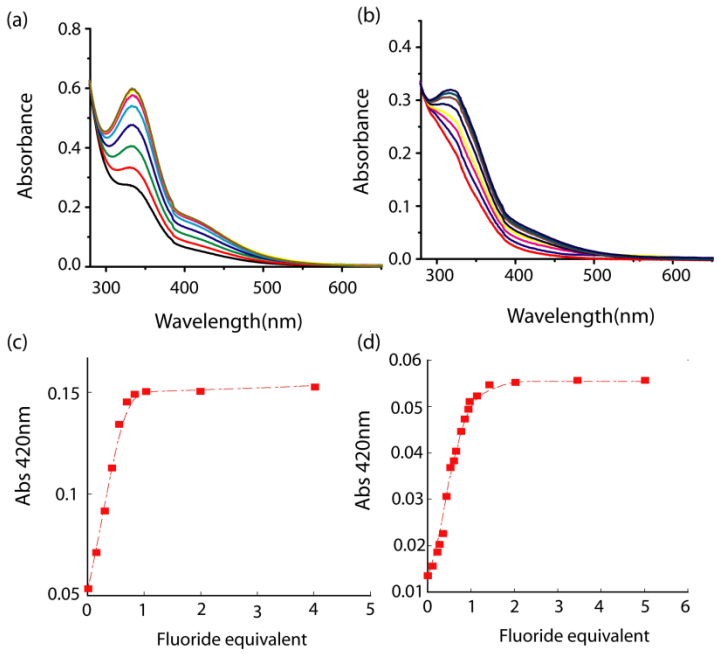

Fig. S15 a) UV–vis titration of the receptor L1(4.0 x 10^{-5} M) in DMSO–H_2O (5 : 1) (v/v) solution with standard solution of [*n*−Bu_4N]F. (b) The change of UV-vis spectra of the receptor L2 (3.4 x 10^{-5} M) in DMSO–H_2O (5 : 1) (v/v) solution upon addition of standard solution of [*n*−Bu_4N]F. (c) (c) Relative change in the absorbance of L1 (4.0 x 10^{-5} M) at 420 nm upon addition of fluoride anions in DMSO–H_2O (5 : 1) (v/v). (d) Plot of the change in the absorbance at 420nm of L2 upon addition of fluoride in DMSO–H2O (5 :1) (v/v).

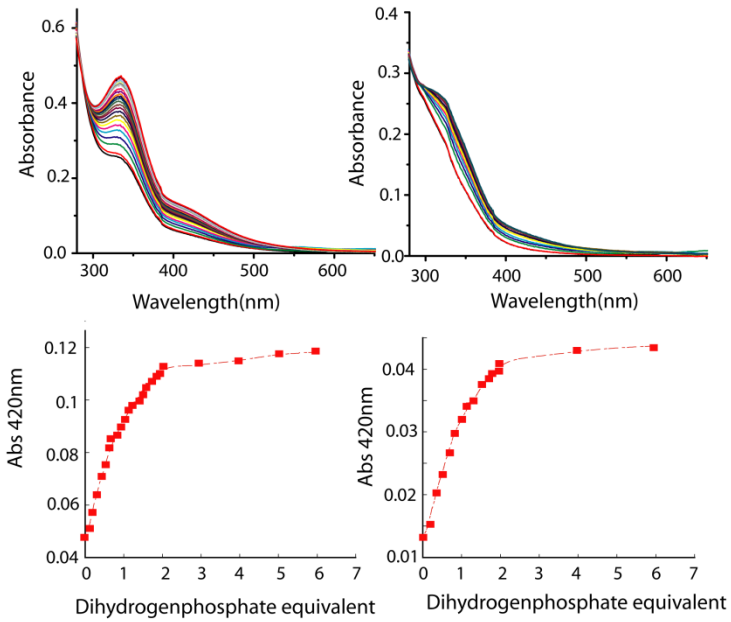

Fig. S16 a) UV–vis titration of the receptor L1(4.0 x 10^{-5} M) in DMSO–H_2O (5 :1) (v/v) solution with standard solution of [*n*-$Bu_4N]H_2PO_4$. (b) The change of UV-vis spectra of the receptor L2 (3.4 x 10^{-5} M) in DMSO–H_2O (5 :1) (v/v) solution upon addition of standard solution of [*n*-$Bu_4N]H_2PO_4$. (c) (c) Relative change in the absorbance of L1 (4.0 x 10^{-5} M) at 420 nm upon addition of di-hydrogenphosphate anions in DMSO–H_2O (5 :1) (v/v). (d) Plot of the change in the absorbance at 420nm of L2 upon addition of di-hydrogenphosphate in DMSO–H2O (5 :1) (v/v).

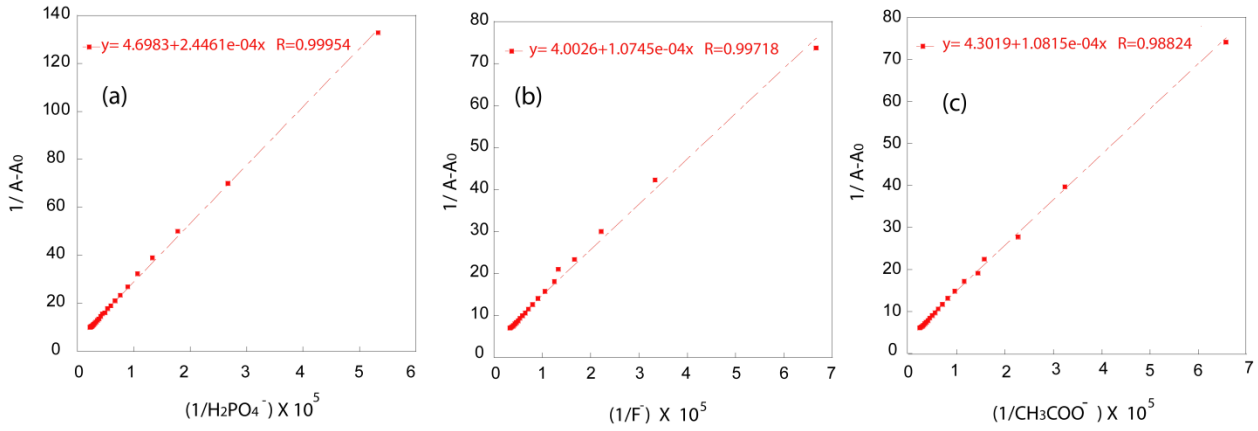

Fig. S17 Benesi–Hildebrand plots of L1 in CH_3CN with (a) Di-hydrogenphosphate, (b) Fluoride (c) Acetate.

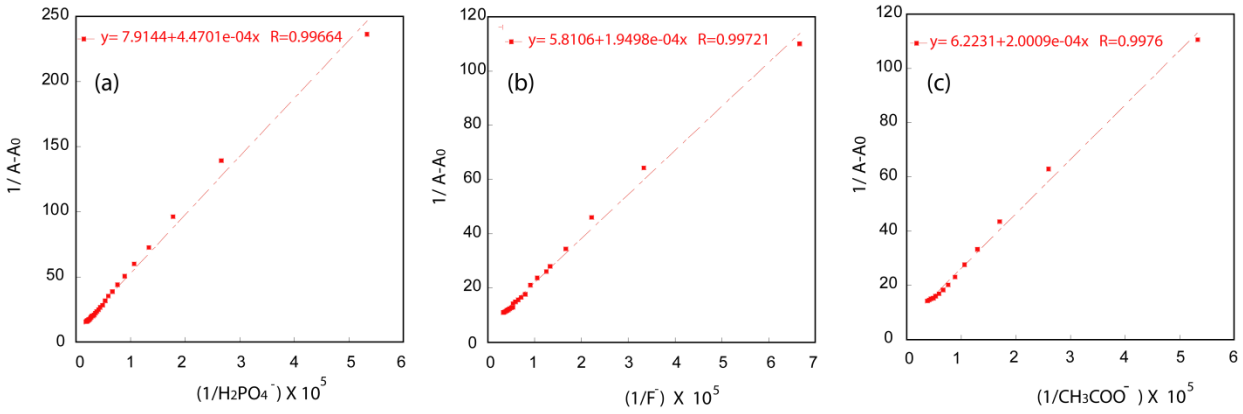

Fig. S18 Benesi–Hildebrand plots of L2 in CH_3CN with (a) Di-hydrogenphosphate, (b) Fluoride (c) Acetate.

Fig.S19. Hydroxide induce step-wise color changes observed for receptor L1.

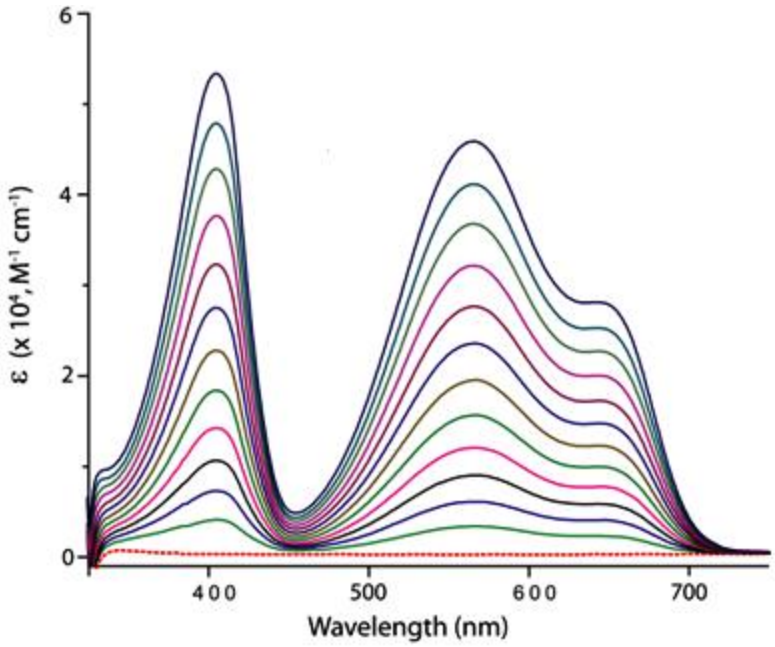

Figure S20. UV-Vis absorption titration of L_C (10 μM) in CH_3CN upon addition of standard hydroxide solution (10 mM). (Figure reproduced from S. K. Dey and G. Das, *Chem. Commun*., 2011, **47**, 4983–4985).

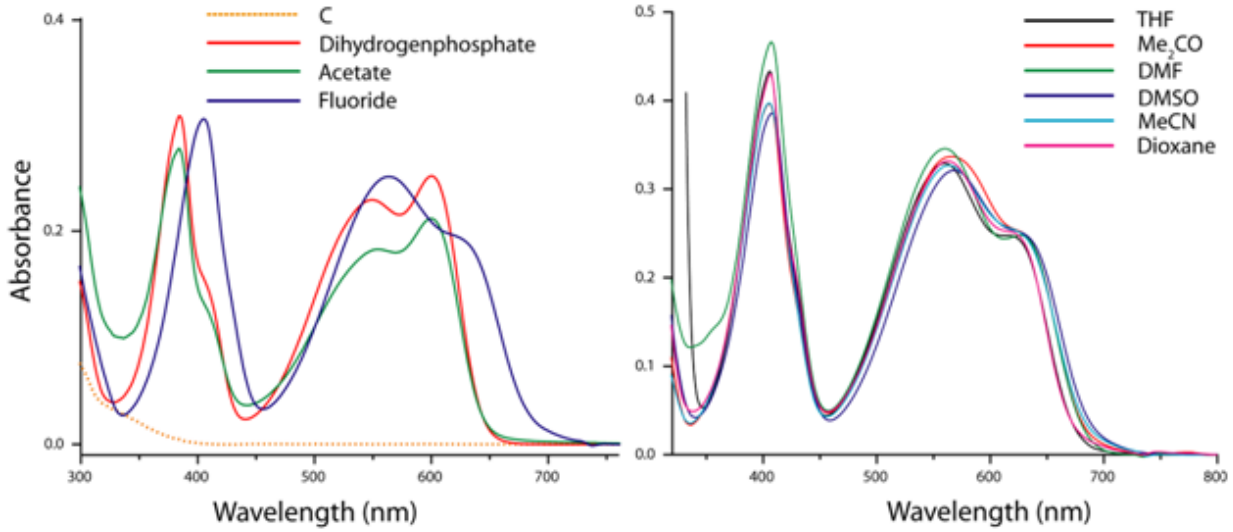

Figure S21. Changes in the UV-vis spectrum of L_C in acetonitrile solution upon addition of TBA salts of strongly basic anions such as, fluoride, acetate and dihydrogenphosphate anions (left) and no observable changes have been observed in the UV-vis spectrum of L_C in various aprotic solvents upon addition of TBAOH salt (right). (Figure reproduced from S. K. Dey and G. Das, *Chem. Commun*., 2011, **47**, 4983–4985).

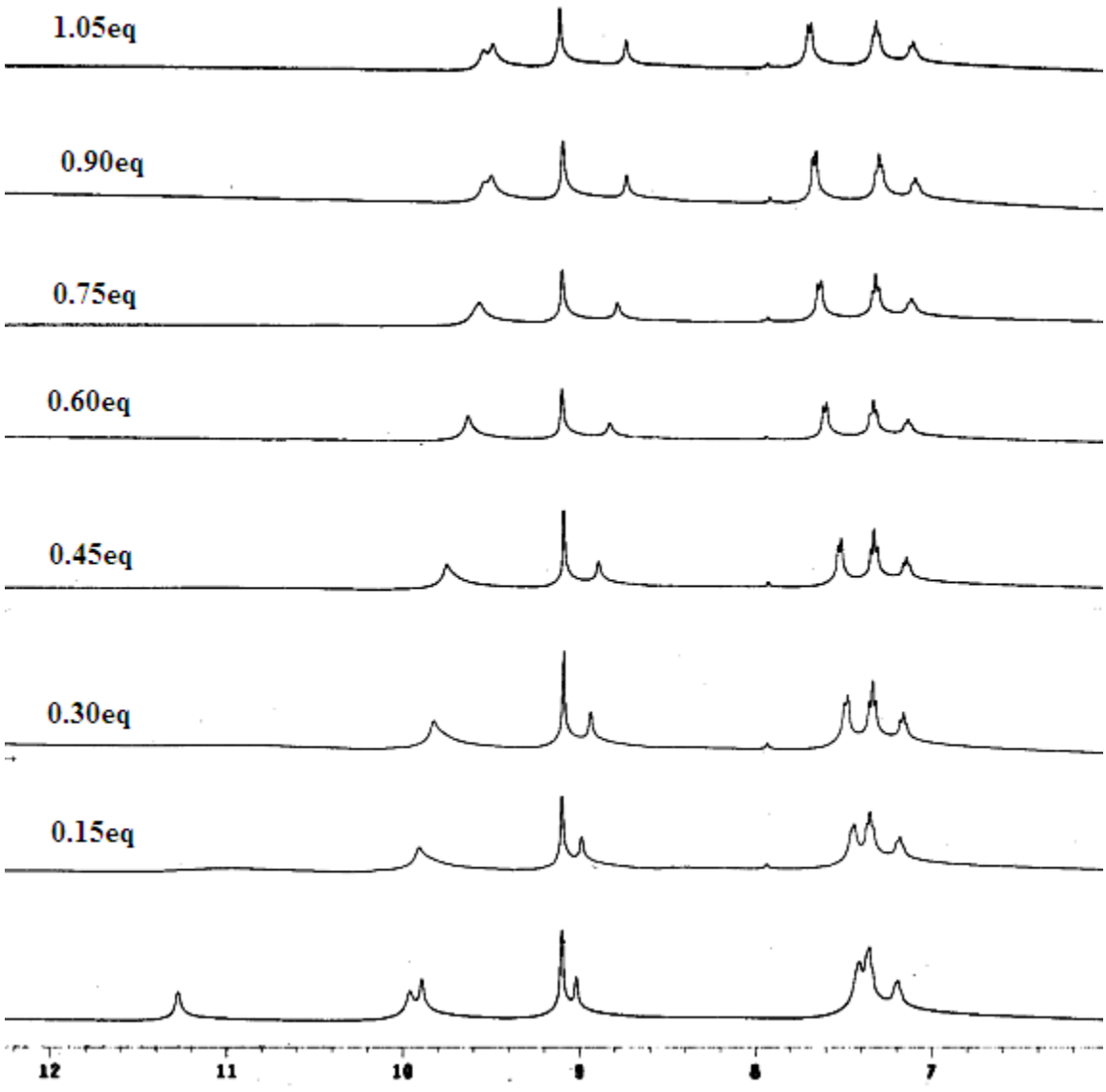

Fig. S22 Stack plot of the ^{1}H NMR spectra of receptor L1 in the presence of increasing amounts of [*n*−Bu_4N]F recorded in d_6-DMSO at 298 K.

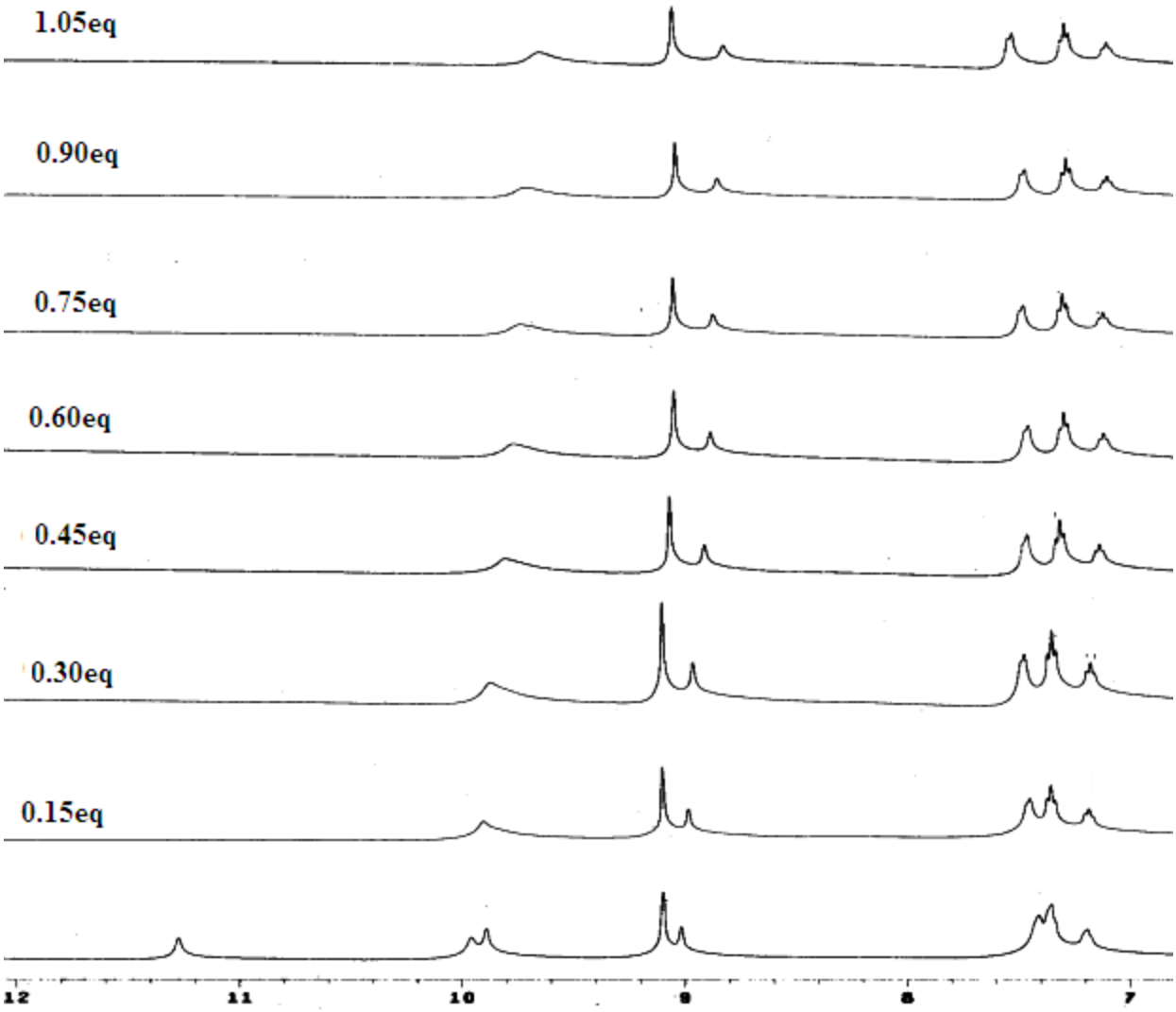

Fig. S23 Stack plot of the ^{1}H NMR spectra of receptor L1 in the presence of increasing amounts of [*n*−Bu_4N]H_2PO_4recorded in d_6-DMSO at 298 K.

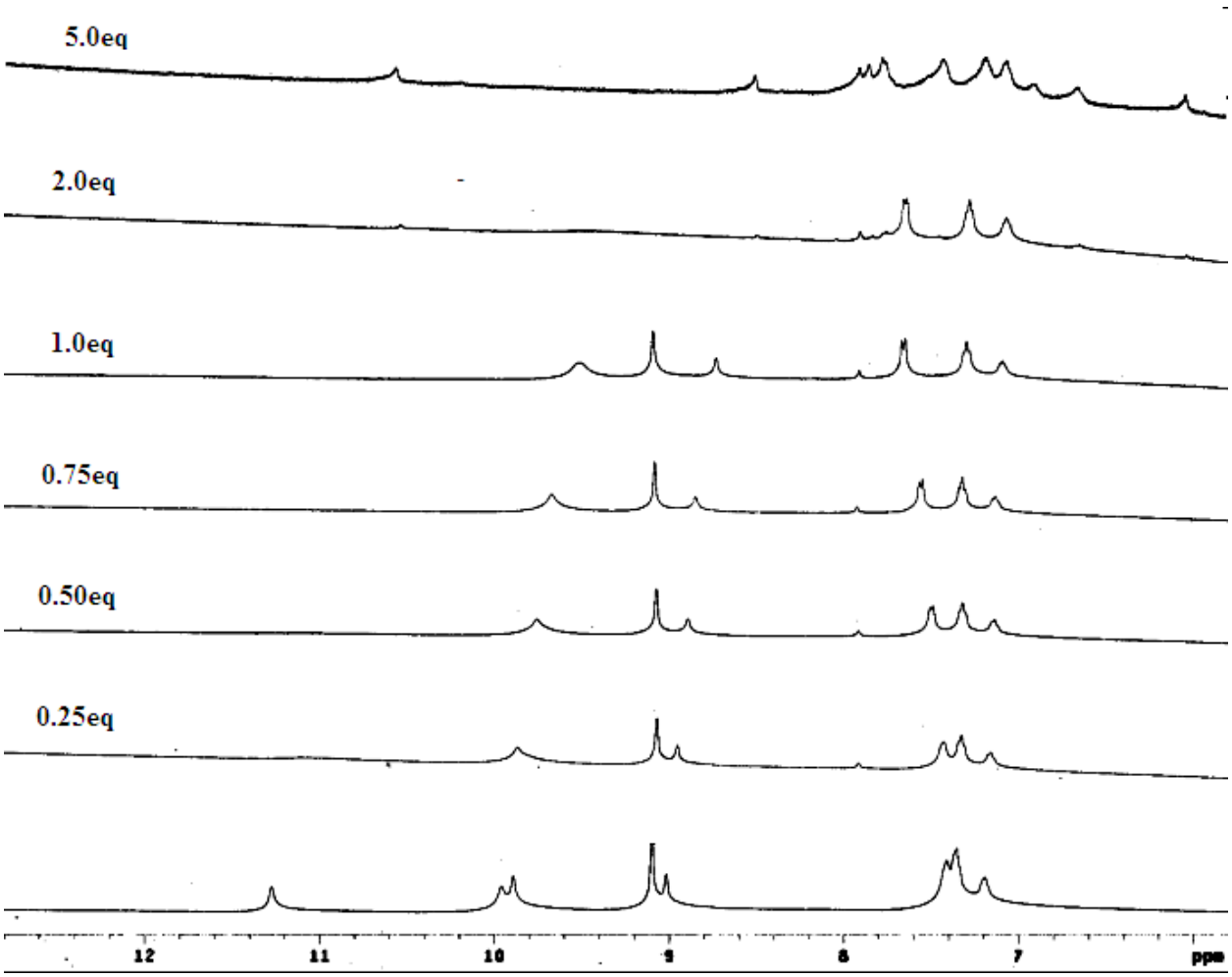

Fig. S24 Stack plot of the ^{1}H NMR spectra of receptor L1 in the presence of increasing amounts of [*n*−Bu_4N]OH recorded in d_6-DMSO at 298 K.

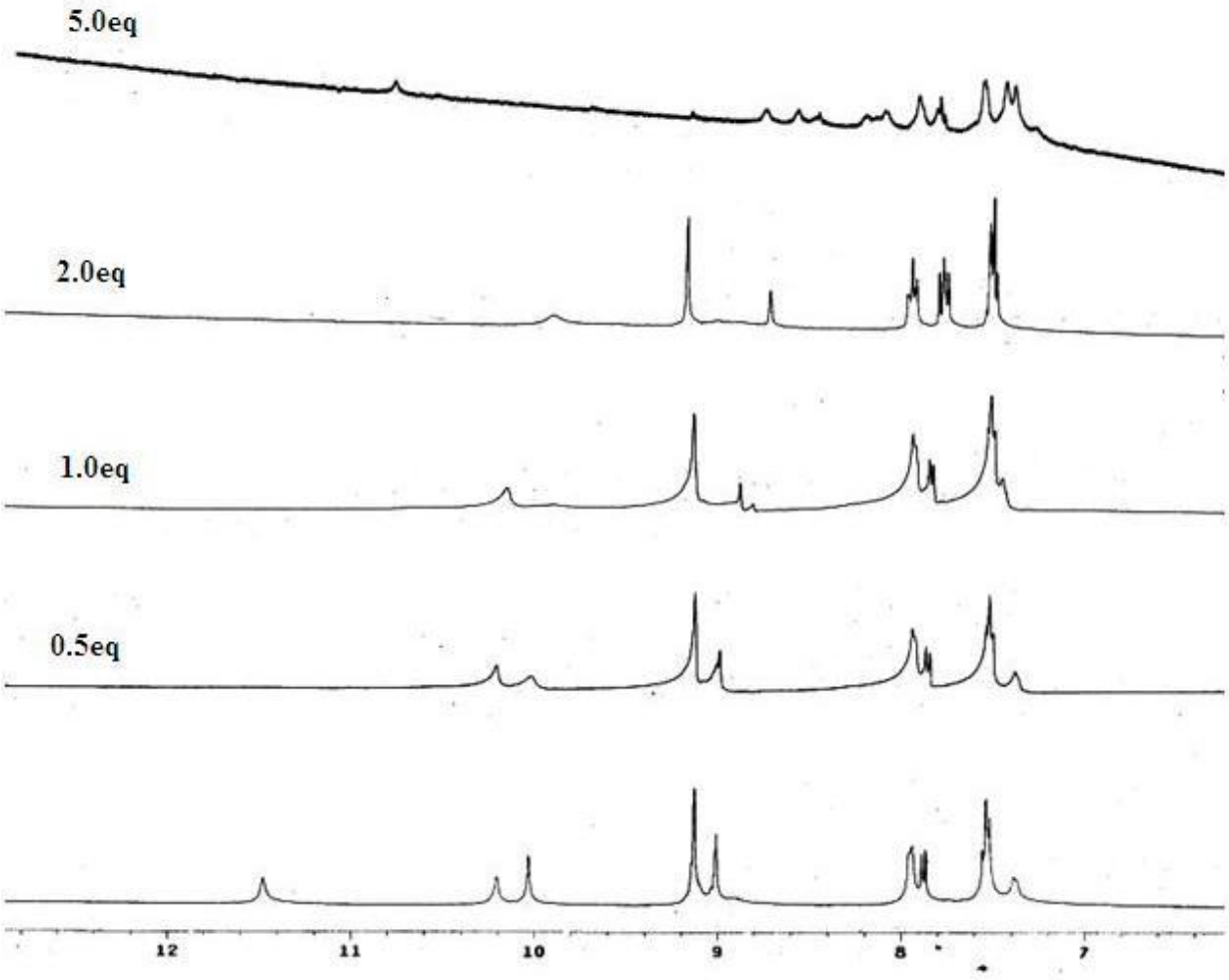

Fig. S25 Stack plot of the ^{1}H NMR spectra of receptor L2 in the presence of increasing amounts of [*n*−Bu_4N]OH recorded in d_6-DMSO at 298 K.

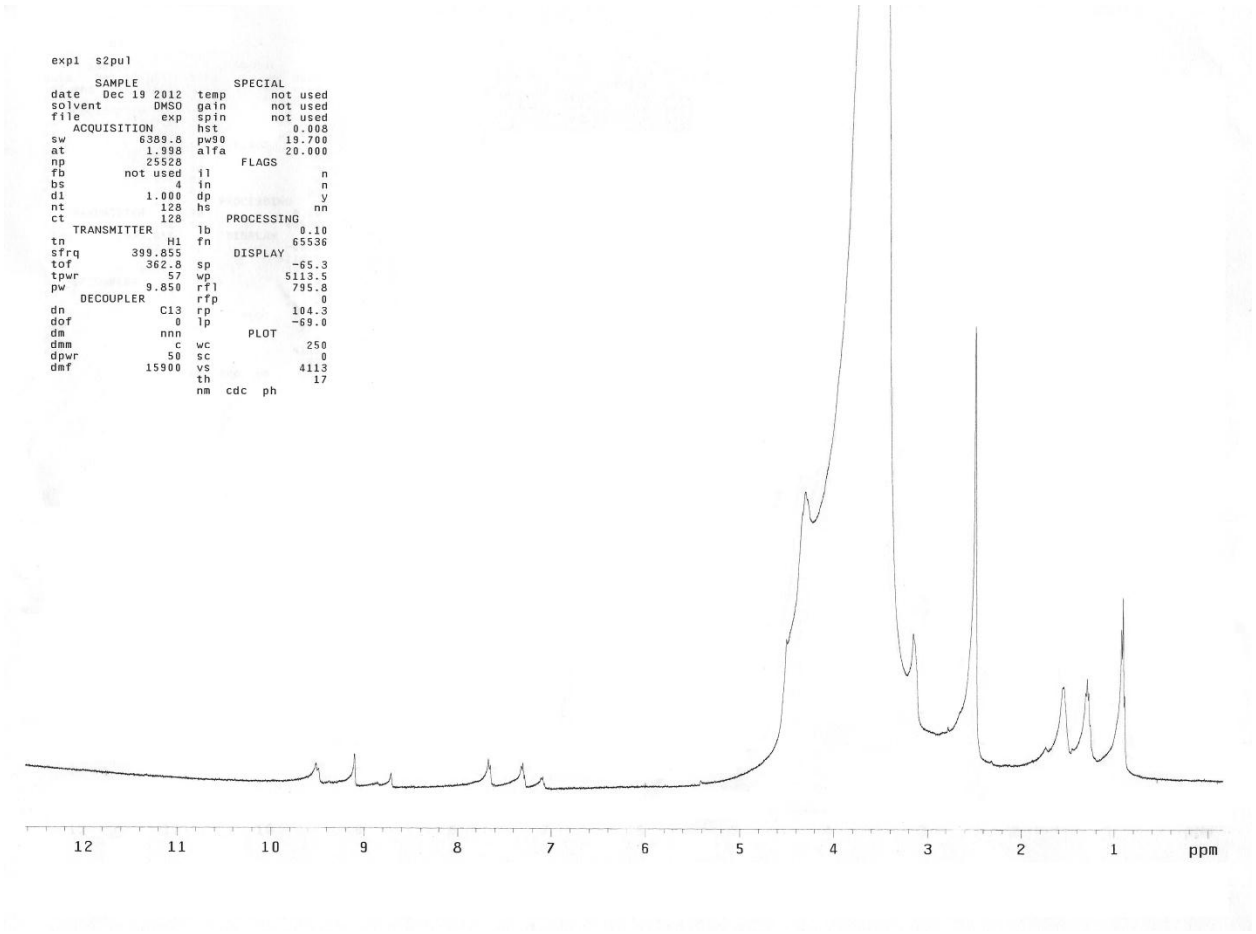

Fig.S26 ^{1}H-NMR spectrum of Salt 1 ind_6-DMSO at 298K

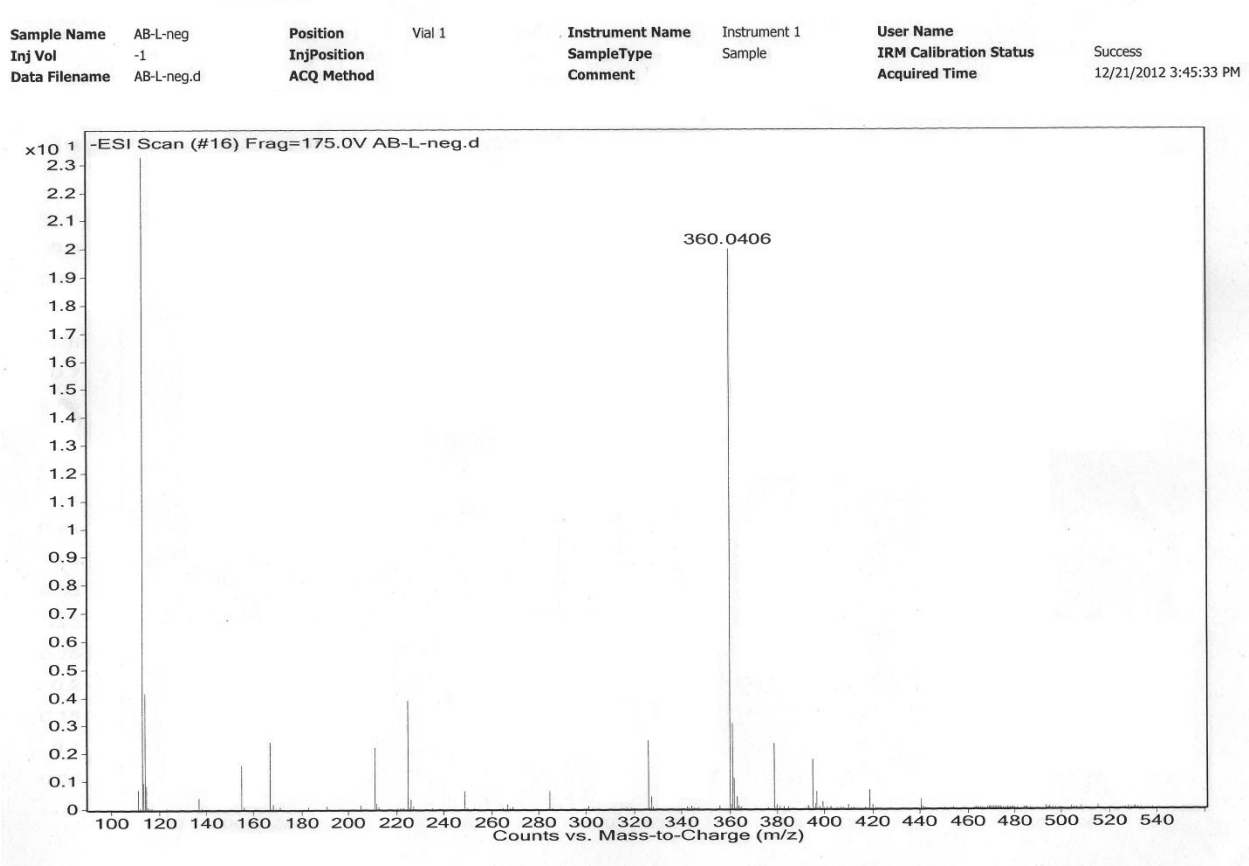

Fig.S27 Mass spectrum of Salt 1 in acetonitrile**.**

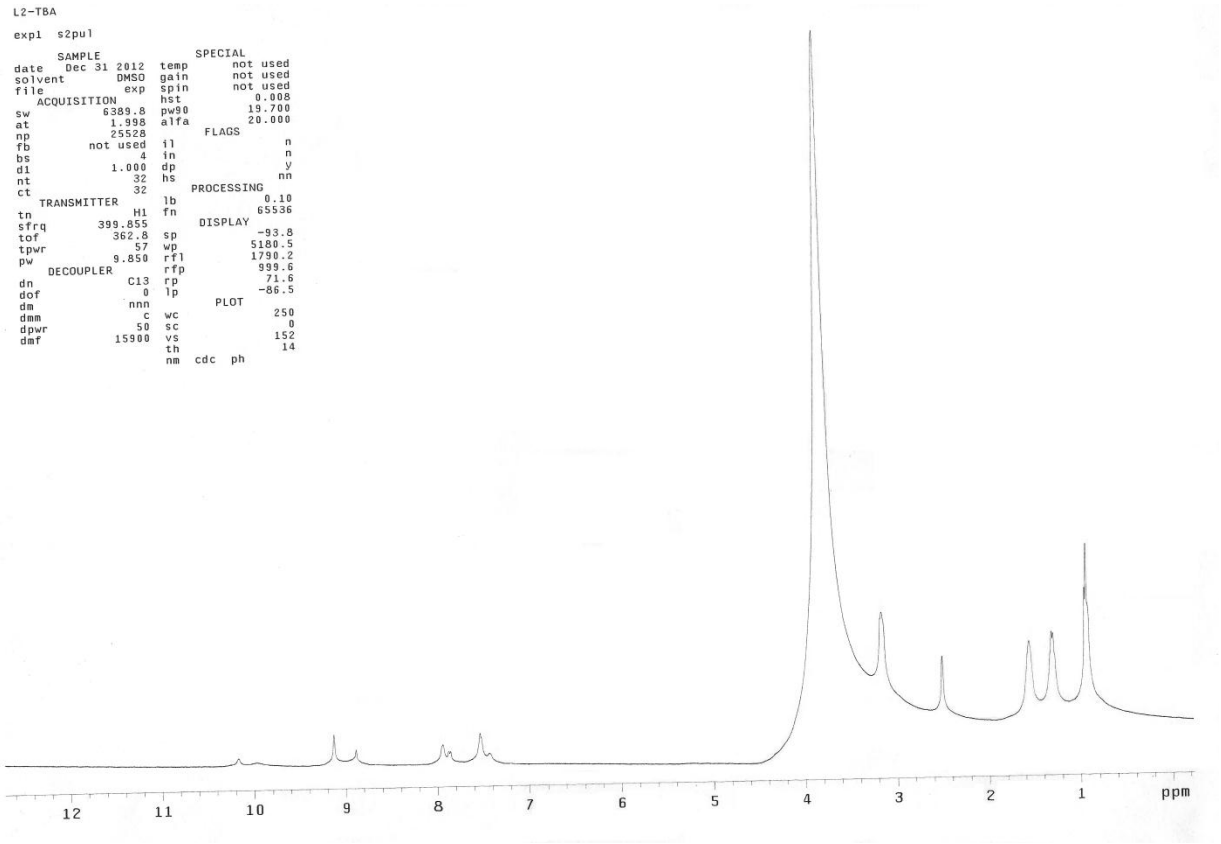

Fig.S28 ^{1}H-NMR spectrum of Salt 3 ind_6-DMSO at 298K.

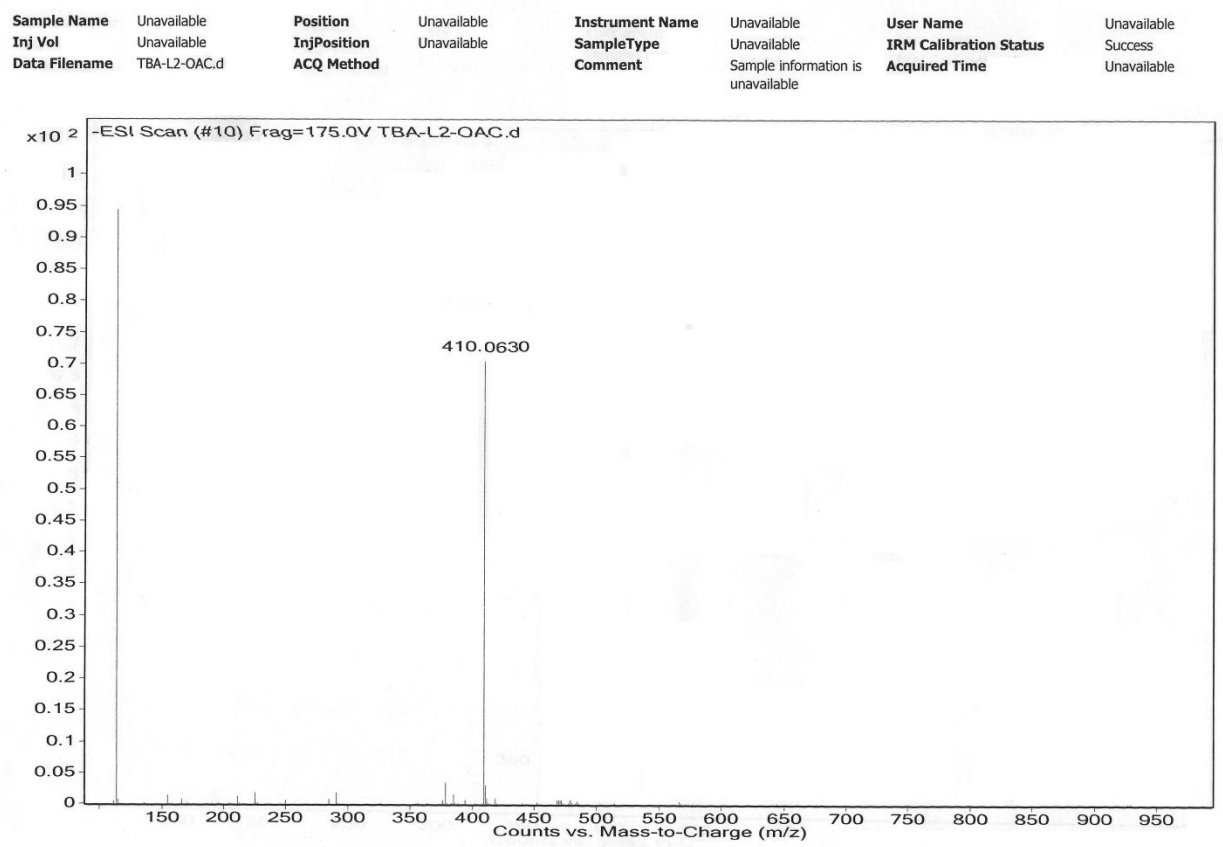

Fig.S29 Mass spectrum of Salt 3 in acetonitrile**.**